OPEN ACCESS

University of BRISTOL

Green, K., Krauskopf, B., & Lenstra, D. (2006). Mode structure of a vertical-cavity surface-emitting laser subject to optical feedback.

Link to publication record in Explore Bristol Research
PDF-document

Mode structure of a vertical-cavity surface-emitting laser subject to optical feedback

K. Green[1], B. Krauskopf[2] and D. Lenstra[3]

[1]Quantum Electronics Theory and Laser Centre, Vrije Universiteit Amsterdam, The Netherlands
[2]Department of Engineering Mathematics, University of Bristol, UK
[3]Faculty of Electrical Engineering, Mathematics and Computer Science,
Delft University of Technology, The Netherlands

We present an analysis of the external cavity mode (ECM) structure of a vertical-cavity surface-emitting laser subject to optical feedback. We consider a model in which two transverse optical modes are excited. Furthermore, we allow weak coupling of the modes via the feedback term. (In addition to the coupling through the inversion.) We use numerical continuation techniques to find and follow solutions of the governing partial, delay differential equations. This approach allows us to show how the ECM structure depends on the key parameters of feedback strength, feedback phase and the amount of coupling via the feedback term.

Vertical-cavity surface-emitting lasers (VCSELs) can support a number of transverse optical modes. Under external influence, such as pump modulation [1], optical injection [2] or optical feedback [3], these modes may interact resulting in complex dynamics. In this study, we investigate a VCSEL model in which the first two, rotationally symmetric, linearly polarised optical modes (LP_{01} and LP_{02}) are excited [3]. We include a general form of optical feedback in which the electric fields of the two modes can couple via the external-cavity round-trip. This is in contrast to previous studies in which each field receives feedback only from itself [3]. More specifically, we study the external-cavity mode (ECM) structure of a VCSEL with a small amount of feedback induced cross-coupling between the electric fields. The ECMs underpin the more complicated dynamics and, as such, a detailed analysis of their dependence on parameters is needed to fully understand a VCSEL subject to optical feedback.

In dimensionless form, our VCSEL model [1] can be described by the following system of delayed partial differential equations

$$\frac{dE_n}{dt} = (1+i\alpha)\left[\int_0^1 \psi_n N\, r dr\right] E_n + \kappa F_n(t,\tau)e^{iC_p}, \quad n=1,2, \tag{1}$$

$$T\frac{\partial N}{\partial t} = d_f\left[\frac{1}{r}\frac{\partial}{\partial r}\left(r\left(\frac{\partial N}{\partial r}\right)\right)\right] - N + J - \sum_{n=1,2}\left(\left(1+2\left[\int_0^1 \psi_n N\, r dr\right]\right)\psi_n|E_n|^2\right) \tag{2}$$

describing the evolution of the two complex electric fields $E_1(t)$ and $E_2(t)$, associated with the radial profiles $\psi_1(r)$ and $\psi_2(r)$ of the LP_{01} and LP_{02} modes, respectively, and the evolution of the spatial carrier distribution $N(r,t)$. Dimensionless parameters are the linewidth enhancement factor $\alpha = 3.0$, the diffusion coefficient $d_f = 0.05$, the ratio between the carrier lifetime and the photon decay rate $T = 750.0$, the pump applied to the cladding region $J_{\min} = 0.0$ and to the core (with radius $a = 0.3$) region $J_{\max} = 2.0$. This value of pump current was chosen well above threshold so that the system is lasing. The
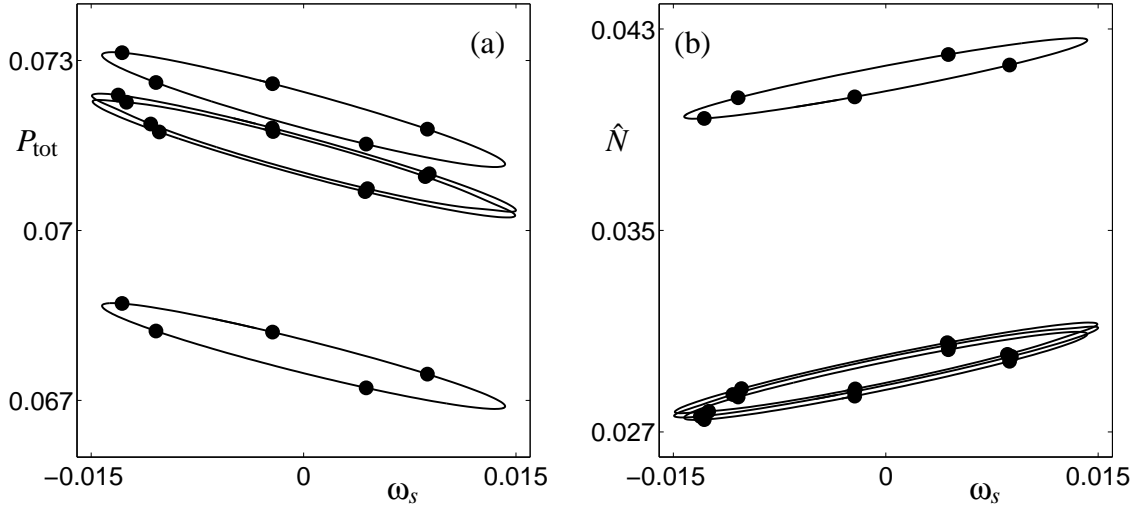
Figure 1: ECM-components for $\eta = 0.9$ with ECMs for $C_p = 0$, shown in the $(\omega_s, P_{\text{tot}})$-plane (a) and the $(\omega_s, \hat{N})$-plane (b).

feedback terms $\kappa F_n(t, \tau)e^{iC_p}$ involve the dimensionless (weak) feedback rate $\kappa = 0.005$, and the dimensionless propagation time $\tau = 500$ between the VCSEL and an external reflector; corresponding to a physical distance of approximately 10 cm. Furthermore, C_p represents the feedback phase, which can be controlled experimentally by varying the length of the external cavity on the scale of the optical wavelength, so that τ remains unchanged [6].

In past studies the feedback function in Eq. (1) has been given as $F_n(t, \tau) = E_n(t - \tau)$. In other words, there is no coupling of the two electric fields through optical feedback. In this study, we consider the following, more general, feedback terms

$$
\begin{aligned}
F_1(t, \tau) &= \eta E_1(t - \tau) + (1 - \eta)E_2(t - \tau)e^{i\Delta}, & (3) \\
F_2(t, \tau) &= (1 - \eta)E_1(t - \tau)e^{-i\Delta} + \eta E_2(t - \tau). & (4)
\end{aligned}
$$

This allows the two fields to couple through the external-cavity round-trip. The amount of coupling is given by the *coupling parameter* η. For $\eta = 1$, Eqs. (3) and (4) reduce to the zero-coupling case, that is, both fields receive feedback only from themselves. Conversely, for $\eta = 0$, the electric fields are cross-coupled, that is, the first electric field receives feedback from the second field, and vice versa. Finally, we note that Δ describes the difference between the optical frequencies of the two fields in the absence of feedback. In this study, we fix $\Delta = 0$.

In order to employ numerical methods, we first need to discretise (2) in the radial direction r. To this end, we consider 100 intervals, over the radius of the VCSEL, that is, $r \in [0, 1]$. At $r = 0$ we use zero Neumann boundary conditions, and at $r = 1$ we use zero Dirichlet boundary conditions. This results in a large-scale delay differential equation (DDE) of size 105, which presents quite a challenge for an analytical investigation. In fact, even simulated results obtained from direct numerical integration of Eqs. (1) to (4) are very time-consuming to produce. In this study, we use numerical continuation techniques which allow us to find and follow in parameters branches of steady state solutions, irrespective of their stability [7, 5]. These techniques are not generally used for systems
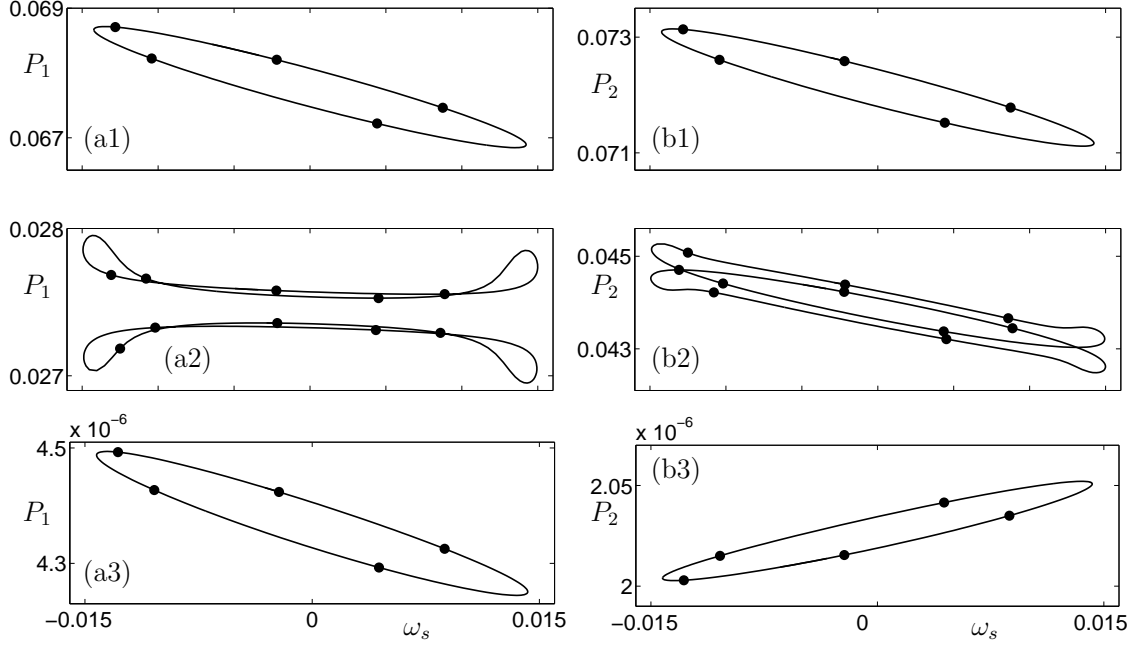
Figure 2: ECM-components for $\eta = 0.9$ with ECMs for $C_p = 0$, shown in the (ω_s, P_1)-plane (a1) to (a3), and (ω_s, P_2)-plane (b1) to (b3).

of this size and, hence, this study also acts as a test-case for the efficiency of such tools in analysing large-scale DDEs.

The basic steady state solutions of Eqs. (1) to (4) are the so-called *external cavity modes* (ECMS). They are given as

$$(E_1(t), E_2(t), N(r,t)) = (R_1 e^{i\omega_s t}, R_2 e^{i\omega_s t + i\Phi}, N_s(r)), \tag{5}$$

where $R_n = |E_n|$ $(n = 1, 2)$ are the amplitudes of the two fields, ω_s is the frequency of the output light, Φ is a fixed phase difference, and $N_s(r)$ is a fixed level of inversion in both space and time. Note that the field intensities are given as $P_1 = R_1^2$ and $P_1 = R_2^2$. We denote the total field intensity as $P_{\text{tot}} = P_1 + P_2$, that is, $P_{\text{tot}} = |E_1|^2 + |E_2|^2$.

Typically, in finding the steady state solutions of lasers with feedback [4], one first finds an analytical expression for the frequency ω_s which is used to obtain the values of amplitude, inversion and phase difference. However, due to its spatial nature, this approach is not possible when solving for the ECMs of Eqs. (1)–(4). Therefore, we turn to the aforementioned numerical continuation techniques.

As for conventional optical feedback (COF) [6] and filtered optical feedback (FOF) [4], a continuous change of the feedback phase C_p over 2π traces the path from one ECM of Eq. (5) to the next. Using the continuation package DDE-BIFTOOL [7] with C_p as a free parameter, we can trace out closed curves on which the steady-state ECM solutions of Eqs. (1) to (4) lie. We refer to these closed curves as the *ECM-components*.

Figure 1 shows the ECM-components of Eqs. (1)–(4) and the ECMs for $C_p = 0$ (shown as large dots). The cross-coupling parameter was fixed at $\eta = 0.9$. Panel (a) shows the ECM-components in the $(\omega_s, P_{\text{tot}})$-plane, and panel (b) shows them in the $(\omega_s, \hat{N})$-plane, where $\hat{N}$ is the mean value of $N(r)$ over the radial distance $r \in [0, 1]$. The laser's intensity

and inversion are in direct competition with one another. For example, the lower solutions in Fig. 1(a) correspond to the upper solutions in Fig. 1(b). Furthermore, for our parameter choice, the ECMs are shown to lie on four separate ECM-components which, like for the COF laser, have the shape of an ellipse. (For the COF laser, one always finds a single ECM-component.)

Figure 2 shows the same ECM-components for $\eta = 0.9$ and ECMs for $C_p = 0$ but now in terms of the intensity contributions of the individual fields P_1 (a1)–(a3) and P_2 (b1)–(b3). Three panels are used due to the position of the ECM-components on the y-axes. We now find that, while the ECM-components shown in Fig. 1(a) have similar values of total intensity P_{tot}, the individual intensities of the two fields E_1 and E_2 can be quite different. Specifically, we have three types of solutions. In the first, the field E_1 dominates, while E_2 hardly contributes to the total intensity; see the ECM-components shown in Figs. 2(a1) and (b3). These solutions make up the lowermost ellipse shown in Fig. 1(a). Conversely, we have a solution in which the field E_2 dominates, while E_1 hardly contributes to the total intensity. This corresponds to Figs. 2(a3) and (b1), the uppermost ellipse of Fig. 1(a). Finally, we have solutions in which both fields E_1 and E_2 contribute to the total intensity. These solutions lie on the ECM-components shown in Figs. 2(a2) and (b2). They correspond to the two intermediate ellipses of Fig. 1(a).

In summary, it has been shown that, while the total intensities of the ECMs on each of the ECM-components are very similar, the individual contributions of the two fields can be quite different. For example, we find solutions in which one of the two fields hardly contributes to the total intensity. How these ECM-components depend on other parameters, in particular on a variation of κ and η is presently being investigated and will be discussed elsewhere.

References

[1] A. Valle, "Selection and modulation of high-order transverse modes in vertical-cavity surface-emitting lasers", *IEEE J. Quantum Electron.*, vol. 34, pp. 1924–1932, 1998.

[2] J. Y. Law, G. H. M. van Tartwijk, and G. P. Agrawal, "Effects of transverse-mode competition on the injection dynamics of vertical-cavity surface-emitting lasers", *Quantum Semiclass. Opt.*, vol .9, pp. 737–747, 1997.

[3] M. S. Torre, C. Masoller, and P. Mandel, "Transverse-mode dynamics in vertical-cavity surface-emitting lasers with optical feedback", *Phys. Rev. A*, vol. 66, 053817, 2002.

[4] K. Green and B. Krauskopf, "Mode structure of a semiconductor laser subject to filtered optical feedback", *Opt. Commun.*, vol. 258, pp. 243–255, 2006.

[5] B. Krauskopf, "Bifurcation analysis of lasers with delay", in *Unlocking dynamical diversity: Optical feedback effects on semiconductor lasers*, D. M. Kane and K. A. Shore, Eds., Wiley, 2005, pp. 147–183.

[6] T. Heil and I. Fischer and W. Elsäßer and B. Krauskopf and K. Green and A. Gavrielides, "Delay dynamics of semiconductor lasers with short external cavities: Bifurcation scenarios and mechanisms", *Phys. Rev. E*, vol. 67, 066214, 2003.

[7] K. Engelborghs, T. Luzyanina, and D. Roose, "Numerical bifurcation analysis of delay differential equations using DDE-BIFTOOL", *ACM Trans. Math. Softw.*, vol. 28, pp. 1–21, 2002.